



Prediction of Absolute Solvation Free Energies using Molecular Dynamics Free Energy Perturbation and the OPLS Force Field

Devleena Shivakumar,^{*,†} Joshua Williams,[‡] Yujie Wu,[†] Wolfgang Damm,[†]
John Shelley,[‡] and Woody Sherman[†]

*Schrödinger, Inc., 120 West 45th Street, 17th Floor, New York, New York 10036 and
101 SW Main Street, Suite 1300, Portland, Oregon 97204*

Received November 4, 2009

Abstract: The accurate prediction of protein–ligand binding free energies is a primary objective in computer-aided drug design. The solvation free energy of a small molecule provides a surrogate to the desolvation of the ligand in the thermodynamic process of protein–ligand binding. Here, we use explicit solvent molecular dynamics free energy perturbation to predict the absolute solvation free energies of a set of 239 small molecules, spanning diverse chemical functional groups commonly found in drugs and drug-like molecules. We also compare the performance of absolute solvation free energies obtained using the OPLS_2005 force field with two other commonly used small molecule force fields—general AMBER force field (GAFF) with AM1-BCC charges and CHARMM-MSI with CHelpG charges. Using the OPLS_2005 force field, we obtain high correlation with experimental solvation free energies ($R^2 = 0.94$) and low average unsigned errors for a majority of the functional groups compared to AM1-BCC/GAFF or CHelpG/CHARMM-MSI. However, OPLS_2005 has errors of over 1.3 kcal/mol for certain classes of polar compounds. We show that predictions on these compound classes can be improved by using a semiempirical charge assignment method with an implicit bond charge correction.

Introduction

The accurate determination of free energies (solvation and binding) has been a primary objective for computational methods since the inception of molecular modeling and computer-aided drug design.^{1,2} The solvation free energy is a critical component of many important problems in the fields of chemistry, biology, and pharmaceutical sciences, such as protein folding, conformational transitions, protein–ligand binding, and transport of drugs across biological membranes.^{3,4} Hence, a large number of studies in the literature have focused on the quantitative determination of solvation free energies. Furthermore, the prediction of solvation free energies provides an excellent opportunity for the testing of methods and force fields.

Although the concept and underlying theory of free energy calculations were laid out several decades ago,^{5,6} free energy calculations have not been used routinely in drug discovery for three main reasons. First, free energy calculations are notoriously complicated to set up and take a lot of effort even for experts. Additionally, they are computationally expensive, often taking days of processor time even for a single calculation. Finally, the accuracy of the methodology applied to pharmaceutically relevant systems has not been systematically validated across a broad range of targets and ligands. The former two problems have been partly solved by the availability of automated free energy perturbation (FEP) and thermodynamic integration (TI) workflows within modern molecular dynamics (MD) and Monte Carlo (MC) software packages and by the continued growth (in number and speed) of accessible computational resources. The systematic validation across diverse and relevant systems remains a limitation and is one of the primary focuses of our group and others in the field.

* Corresponding author. Telephone: 646-366-9555. Fax: 646-366-9551. E-mail: devleena.shivakumar@schrodinger.com.

[†] Schrödinger, Inc., New York, New York.

[‡] Schrödinger, Inc., Portland, Oregon.

The calculation of absolute solvation free energies is a more tractable problem than predicting binding free energies, since the solvent molecules equilibrates more quickly around a small organic solute than around the binding site of the protein, and there are fewer internal degrees of freedom to consider with a small molecule than with a protein–ligand complex. Since absolute solvation free energies have been experimentally determined for hundreds of small molecules, it allows for a direct comparison between the experimental and calculated values. Also, several groups have published calculated absolute solvation free energies, making it possible to compare the performance of various methodologies and force fields.

There are many physics-based methods available to calculate solvation free energies. Often a compromise has to be made between the speed and the accuracy of the model. At one end of the spectrum are methods that use continuum solvation models, such as generalized Born (GB)^{7,8} and Poisson–Boltzmann (PB) models,^{9–11} which are computationally efficient but neglect the role of explicit water molecules. On the other hand, explicit solvent models are considered to be more rigorous because they more closely represent the underlying physical system of interest. However, explicitly modeling solvent molecules adds to the computational cost and complexity of the simulations. The FEP or TI that are coupled to MD or MC computer simulations are commonly used to compute solvation free energies.^{12,13} The first successful FEP calculations of relative solvation free energies were published in 1985 by Jorgensen and Ravimohan, who computed the difference between ethane and methanol using MC simulations and found excellent agreement with experiment.¹⁴

Recent studies have compared the performance of explicit solvent MD/FEP in predicting absolute solvation free energies for a few hundred small molecules using various force fields and solvent models.^{15–18} A study comparing the accuracy of different implicit solvent models using MD/FEP calculations on a set of 504 neutral small molecules using GROMACS 3.3 MD simulation package¹⁹ reported root mean square (rms) errors ranging from 2.01 to 2.43 kcal/mol, depending on the implicit solvent model, and correlation coefficients (R^2) from 0.69 to 0.77.¹⁶ The same group reported an rms error of 1.26 kcal/mol, a correlation coefficient of 0.89, and a mean error of 0.68 for the same set of molecules using explicit solvent and the general AMBER force field (GAFF)²⁰ with partial charges from the Austin Model 1 using bond charge corrections (AM1-BCC). Another study by Shivakumar et al.¹⁸ used a set of 239 neutral small molecules to compare implicit versus explicit solvent molecules using two popular small-molecule general atom force fields, GAFF²⁰ and CHARMM-MSI,²¹ along with various charge models, such as semiempirical AM1-BCC²² and quantum chemical charge methods, such as CHarges from ELECtrostatic Potentials using a Grid-based method (CHelpG)²³ and Restrained Electrostatic Surface Potential fit (RESP).²⁴ The results from this study also showed that the best

results were obtained with the AM1-BCC/GAFF combination, having a correlation coefficient of 0.87.

Here, we extend the work reported by Shivakumar et al.¹⁸ by using the OPLS_2005 force field to compute absolute solvation free energies for the same set of 239 neutral small molecules and to compare the results to those previously obtained with the GAFF and CHARMM-MSI. We also discuss the use of an improved semiempirical charge assignment method based on the CM1A procedure of Cramer and Truhlar along with implicit bond charge correction terms, called CM1A-BCC, to improve the solvation free energy predictions for polar molecules.²⁵ Our ultimate goal is to extend the application of MD/FEP to calculate relative binding free energies of congeneric molecules to pharmaceutically relevant targets, which will be addressed in future work.

Theory

Molecular Dynamics/Free Energy Perturbation (MD/FEP). The MD/FEP simulations were carried out using the Desmond MD package, version 20108, as distributed by Schrödinger.^{26–28} Desmond is a relatively new MD engine developed by D. E. Shaw Research and can be used to run a variety of molecular simulations, including minimization, standard MD, simulated annealing, and replica exchange (REMD) simulations, in addition to FEP. Desmond implements a number of novel algorithmic optimizations that are explained in detail elsewhere,^{28–31} such as minimizing interprocessor communication, ensuring conservation of energy even with single precision calculations, and computing long-range electrostatic interactions in the Fourier space with a smooth particle mesh Ewald³² implementation.

Total Free Energy. The FEP method allows one to compute the change in free energy of a chemical system as it evolves from state A to state B. The computation is essentially based on Zwanzig's equation:⁶

$$\Delta G_{A \rightarrow B} = -k_B T \ln \langle \exp(-(U_B - U_A)/k_B T) \rangle_A \quad (1)$$

where k_B is the Boltzmann constant, T is the absolute temperature, U_A and U_B are the potential energies of the A and B states, respectively, and the $\langle \dots \rangle_A$ denotes the ensemble average over configurations sampled from the A state. For absolute solvation free energy calculations, we can define A as the solute molecule in the gas phase and B as the solute molecule in the solution phase. Solvation is, thus, regarded as a transfer process where the solute molecule enters the solvent from the ideal gas. It is worth noting that the ΔG under this definition is called the *transfer* free energy—the free energy of transferring the solute from ideal gas to aqueous solution of the same concentration.

A thermodynamic cycle for transferring a solute from vacuum to solvent phase is shown in Figure 1. The solvation free energy can be calculated along the vertical line (2a and b in Figure 1), which consists of annihilating or creating the solute molecule both in vacuo and in solvent. This scheme is also known as double annihilation since the solute is

annihilated (or created) from both the vacuum and solution phases (routes 2a and b, respectively, in Figure 1). Since the total free energy change in the thermodynamic cycle must be zero, the following can be deduced

$$\Delta G_{\text{solvation}} = \Delta G_{\text{annihilation}}^0 - \Delta G_{\text{annihilation}}^1 \quad (2)$$

Instead of directly simulating the process in 1a from Figure 1, a common approach is to employ a thermodynamic cycle and compute ΔG for the solvation process by eq 2. An alternative approach is used in Desmond that takes advantage of the fact that we recover the above-defined [solute]_{vacuo} state from [solute]_{solv} by turning off the interactions between the solute and the other molecules. An advantage of this approach is that only one FEP simulation is needed instead of two annihilations. We define the potential of the system as a function of two order parameters, λ_{vdW} and λ_{coul} , to scale the van der Waals (vdW) and electrostatic potentials, respectively, between the solute (M) and the solvent (solv). The total potential ($U(\lambda_{\text{vdW}}, \lambda_{\text{coul}})$) of the system is described by the eq 3:

$$U(\lambda_{\text{vdW}}, \lambda_{\text{coul}}) = U_{\text{M,solv}}^{\text{vdW}}(\lambda_{\text{vdW}}) + U_{\text{M,solv}}^{\text{coul}}(\lambda_{\text{coul}}) + U_{\text{M}}^{\text{bonded}} + U_{\text{M}}^{\text{nonbonded}} + U_{\text{solv}}^{\text{bonded}} + U_{\text{solv}}^{\text{nonbonded}} \quad (3)$$

where $U_{\text{M,solv}}^{\text{vdW}}(\lambda_{\text{vdW}})$ and $U_{\text{M,solv}}^{\text{coul}}(\lambda_{\text{coul}})$ are the vdW and electrostatic potentials between the solute and the solvent, respectively; $U_{\text{M}}^{\text{bonded}}$ and $U_{\text{M}}^{\text{nonbonded}}$ are the bonded and the nonbonded potentials of the solute, respectively; and $U_{\text{solv}}^{\text{bonded}}$ and $U_{\text{solv}}^{\text{nonbonded}}$ are the bonded and the nonbonded potentials of the solvent, respectively. This description recovers the A state for $(\lambda_{\text{vdW}}, \lambda_{\text{coul}}) = 0$ and the B state for $(\lambda_{\text{vdW}}, \lambda_{\text{coul}}) = 1$. For values between 0 and 1, it gives a hybrid system that has scaled similarities to both A and B.

To avoid numerical problems commonly associated with $\lambda_{\text{vdW}} = 0$ for the Lennard-Jones (LJ) 12-6 potential, we use the following soft-core potential:³³

$$U_{\text{M,solv}}^{\text{vdW}}(r, \lambda_{\text{vdW}}) = 4\lambda_{\text{vdW}}\epsilon \left[\left(\frac{\sigma^6}{\alpha(1 - \lambda_{\text{vdW}})^2\sigma^6 + r^6} \right)^2 - \frac{\sigma^6}{\alpha(1 - \lambda_{\text{vdW}})^2\sigma^6 + r^6} \right] \quad (4)$$

α is a positive constant that controls the magnitude of the soft-core term: $\alpha(1 - \lambda_{\text{vdW}})^2\sigma^6$. We used a value of 0.5 for α . Note that this soft-core potential is a function of λ_{vdW} and reduces to the standard LJ potential for $\lambda_{\text{vdW}} = 1$. As

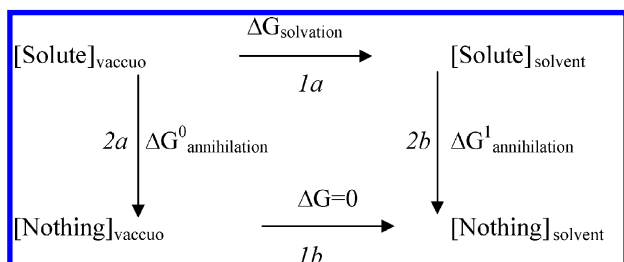


Figure 1. Thermodynamic cycle for calculating absolute solvation free energies.

λ_{vdW} approaches 0, the soft-core term eliminates the problematic singularity in the LJ potential.

A correction term that accounts for the missing long-range dispersion energy due to the cutoff of the vdW potentials³⁴ is also added to the absolute free energy obtained using MD/FEP in Desmond. Assuming a homogeneous solvent beyond the cutoff radius, this term can be analytically obtained as follows:

$$E_{\text{irc}} = -\frac{16\pi\rho}{3r_{\text{cut}}^3} \sum_i \epsilon_{i\text{w}} \sigma_{i\text{w}}^6 \quad (5)$$

where ρ is the water number density of the system, $\epsilon_{i\text{w}}$ and $\sigma_{i\text{w}}$ are LJ parameters for the i -th solute atom and water oxygen atom (water hydrogen atoms do not have LJ interactions for the water models used in this study), the summation is over the solute atoms, and r_{cut} is the cutoff radius for the LJ potential. Adding this correction yields results that are nearly independent of the LJ cutoff distance for reasonable cutoff values at a negligible additional calculation cost.

Bennett Acceptance Ratio Method. We used the Bennett acceptance ratio (BAR) method to estimate the free energy difference from the MD simulations.³⁵ For each window (i), we sampled the potential energy difference in both the forward [$W_i^f = U_{i+1}(x_i) - U_i(x_i)$] and the reverse [$W_i^r = U_{i+1}(x_i) - U_i(x_i)$] directions. The free energy difference ΔG_i between window i and $i+1$ is computed by solving the nonlinear equation:

$$\sum_{j=1}^{L_i} \frac{1}{1 + \frac{L_i}{L_{i+1}} \exp[(W_{ij}^f - \Delta G_i)/k_B T]} - \sum_{k=1}^{L_{i+1}} \frac{1}{1 + \frac{L_{i+1}}{L_i} \exp[(\Delta G_i - W_{i+1,k}^r)/k_B T]} = 0 \quad (6)$$

where L_i is the number of data in the forward or reverse energy ensemble. The statistical uncertainty of ΔG_i for window i was estimated using the subsampling bootstrap method,³⁶ and the total uncertainty is reported as the rms error, RMSE (square root of the sum of the squares of the errors), across all windows.

The OPLS_2005 Force Field. The OPLS_2005 force field, as implemented in the Schrödinger suite 2008, follows the functional form of the OPLS-AA family of force fields with additional stretch, bend, and torsional parameters for better coverage of ligand functional groups.³⁷ The nonbonded parameters are taken from the OPLS-AA force field, which were developed to reproduce heats of vaporizations and densities of pure liquids, are retained as published.^{38–45} The torsional parameters specific to peptides (not relevant in this work) originate from Jensen et al. and Kaminski et al.^{39,40} Stretch and bend parameters for 112 compounds are retained as published, and all other stretch and bend parameters are adjusted to reproduce the structures obtained with quantum mechanics at the B3LYP/6-31G* method and basis set. With the exception of the protein specific parameters, all torsional

parameters were fit to reproduce the conformational energetics obtained from a B3LYP/6-31G* geometry optimization followed by an LMP2/cc-pVTZ(-f) single point energy calculation. The training set used to derive torsional parameters consists of ~660 compounds that are a combination of molecules from papers^{41,45} and a small number of additional compounds.

We also examine the effect of using a semiempirical charge assignment method, called CM1A-BCC, to explore whether predictions can be improved for classes of molecules that present the greatest challenge for the OPLS_2005 force field. The CM1A-BCC charges are obtained from a combination of Cramer–Truhlar’s CM1A charge model²⁵ and fit bond charge correction terms (BCC)⁴⁶ for each atom. The CM1A charge model has been shown to produce accurate solvation free energies,⁴⁷ specifically when used in combination with other force field terms from OPLS-AA.⁴⁸

Methods

The calculations presented in this work were performed using the OPLS_2005 all-atom force field with explicit solvent and were run with the default parameters in the Maestro v8.5 interface to Desmond, version 20108.²⁶ Comparisons to AM1-BCC/GAFF and CHelpG/CHARMM-MSI were made based on previous calculations from Shivakumar et al.¹⁸ The starting 239 neutral small molecules were obtained from Shivakumar et al. and were solvated in an orthorhombic water box using a 10 Å buffer with no ions. All the simulations were run with the SPC water model; however, a subset of simulations was also run with the TIP3P and TIP4P water models for comparison. The solvated structures were minimized for 10 steps with the steepest-descent method followed by a maximum of 1990 steps with the limited memory Broyden–Fletcher–Goldfarb–Shanno (LBFGS) method.⁴⁹ The minimized system was further relaxed with a 24 ps molecular dynamics simulation at 300 K temperature and 1 atm pressure (corresponding to the “quick relaxation” protocol in the Schrödinger interface to Desmond). Finally, production simulations were run for 600 ps for each λ window using the same reference temperature and pressure, which were maintained by chained Nose–Hoover thermostats⁵⁰ and by a Martyna–Tobias–Klein (MTK) barostat.⁵¹ The last 450 ps of each window were used for analysis. All simulations used a 10 Å cutoff radius for both vdW and electrostatic interactions along with smooth particle mesh Ewald³² to calculate long-range electrostatic interactions. The convergence of the final result was checked on a subset of compounds by plotting the variation in RMSE as a function of simulation time (Supporting Information, Figure S1).

λ Schedule. Since free energy is a state function, it is independent of the path taken for the transformation going from state A to state B. However, in practice, the choice of λ schedule determines the precision of the calculated free energy change, as well as the stability of the simulations. The λ schedule used for calculating the absolute solvation free energy in this work has 12 windows (see Table 1) and was devised such that the vdW terms are scaled to full

Table 1. λ Schedule^a

window index	λ_{vdW}	λ_{coul}
1	0.0	0.0
2	0.106974	0.0
3	0.1745536	0.0
4	0.2252634	0.0
5	0.2816288	0.0
6	0.366175	0.0
7	0.5014272	0.0
8	0.7099106	0.0
9	1.0	0.25
10	1.0	0.5
11	1.0	0.75
12	1.0	1.0

^a The λ_{vdW} and λ_{coul} refer to the scaling the vdW and coulombic interactions, respectively, at each window.

Table 2. Functional Group Compound Classification and Number of Compounds in Each Class

type	number	type	number
alkanes	8	esters	15
alkenes	10	ethers	11
alkynes	5	halogen, bromo	10
alcohols	17	halogen, chloroalkanes	11
aldehydes	6	halogen, chloroalkenes	5
aliphatic amines	16	halogen, chloroarenes	3
amides	5	halogen, fluoro	6
arenes	14	halogen, iodo	8
aromatic amines	14	thiols	4
bifunctional amine	3	ketones	12
bifunctional groups	5	multiple halogens	15
branched alkanes	7	nitriles	5
carboxylic acids	5	nitro	7
cycloalkanes	5	sulfides	5
disulfides	2	total	239

strength before the charging of the atoms starts. This prevents atoms of opposite charge from approaching each other closely enough to fall into the attractive singularity in the electrostatic potential. The statistical mechanics of the separation of vdW and electrostatic terms has been discussed in detail in literature by Deng and Roux.⁵² The λ_{vdW} values given in the table were empirically determined by minimizing the variances in free energy predictions for a small set of training molecules (unpublished results). The linear five-step schedule (from 0 to 1) used for λ_{coul} performed well on the small set of training molecules, although the results were fairly insensitive to the details of this schedule (see Results and Discussions Section).

Test Set Selection. We used the same set of 239 small neutral organic molecules as described in Shivakumar et al.^{18,47,53} This allowed for a direct comparison of the results obtained here with other force fields and simulation programs. The test set spans diverse chemical functional groups commonly encountered in drug design (Table 2). These include saturated and unsaturated hydrocarbons, strained rings, conjugated systems, aromatic and heterocyclic rings, and many polar functional groups. All calculations were performed with molecules in their neutralized states, including carboxylic acids and amines. The two-dimensional (2D)

Table 3. Comparison of SPC, TIP3P, and TIP4P Water Models^a

entry ID	title	exp	SPC	TIP3P	TIP4P
13-Compound Subset					
1	1-3-dioxolane	-4.1	-2.50 ± 0.21	-2.83 ± 0.19	-2.51 ± 0.16
2	4-methyl-1H-imidazole	-10.25	-8.50 ± 0.21	-8.30 ± 0.19	-8.24 ± 0.21
3	biphenyl	-2.64	-1.40 ± 0.24	-1.52 ± 0.21	-0.95 ± 0.24
4	butanal	-3.18	-1.80 ± 0.18	-1.80 ± 0.18	-1.48 ± 0.17
5	cyclopropane	0.75	2.18 ± 0.17	2.04 ± 0.15	2.50 ± 0.11
6	diethyldisulfide	-1.54	-1.28 ± 0.18	-1.29 ± 0.25	-1.00 ± 0.18
7	morpholine	-7.17	-5.54 ± 0.25	-5.22 ± 0.22	-5.12 ± 0.22
8	nitrobenzene	-4.12	-2.61 ± 0.19	-2.72 ± 0.19	-2.03 ± 0.19
9	piperazine	-7.4	-7.63 ± 0.21	-7.41 ± 0.22	-8.35 ± 0.26
10	propionic	-6.47	-5.31 ± 0.19	-5.57 ± 0.19	-4.84 ± 0.21
11	propane-2-methoxy-2-methyl	-0.79	-0.44 ± 0.21	-0.43 ± 0.15	-0.39 ± 0.19
12	propionitrile	-3.85	-3.39 ± 0.17	-3.33 ± 0.16	-3.18 ± 0.19
13	trimethylamine	-3.42	-2.35 ± 0.17	-1.74 ± 0.17	-1.50 ± 0.16
	average unsigned error (AUE)		1.08	1.08	1.46
	R^2		0.96	0.96	0.92
	slope		0.96	0.94	0.99
	intercept		0.89	0.82	1.25
Amino Acid Side Chain Analogues					
1	acetamide (Asn)	-9.71	-8.47 ± 0.20	-8.51 ± 0.23	-8.30 ± 0.22
2	phenol (Tyr)	-3.74	-4.64 ± 0.21	-5.40 ± 0.22	-4.07 ± 0.20
3	acetic acid (AspH)	-4.88	-5.44 ± 0.17	-5.53 ± 0.16	-4.80 ± 0.17
4	4-methyl-1H-imidazole (His)	-10.25	-8.50 ± 0.24	-8.44 ± 0.2	-8.25 ± 0.24
5	toluene (Phe)	-0.89	-0.74 ± 0.17	-0.79 ± 0.21	-0.24 ± 0.17
	average unsigned error (AUE)		0.92	1.08	0.89
	R^2		0.95	0.91	0.96
	slope		0.78	1.21	1.17
	intercept		0.96	1.06	0.13

^a Energies are reported in kcal/mol. The experimental (exp) numbers are shown for comparison.

Table 4. Absolute Solvation Free Energies using 5- and 11- λ Coupling Parameter for Electrostatics^a

entry ID	title	exp	λ_{coul}^5	$\lambda_{\text{coul}}^{11}$
1	1-3-dioxolane	-4.10	-2.50 ± 0.21	-2.58 ± 0.17
2	4-methyl-1H-imidazole	-10.25	-8.50 ± 0.21	-8.72 ± 0.19
3	biphenyl	-2.64	-1.40 ± 0.24	-1.48 ± 0.25
4	butanal	-3.18	-1.80 ± 0.18	-1.83 ± 0.18
5	cyclopropane	0.75	2.18 ± 0.17	2.00 ± 0.11
6	diethyldisulfide	-1.54	-1.28 ± 0.18	-1.23 ± 0.19
7	morpholine	-7.17	-5.54 ± 0.25	-5.28 ± 0.20
8	nitrobenzene	-4.12	-2.61 ± 0.19	-2.49 ± 0.14
9	piperazine	-7.40	-7.63 ± 0.21	-7.97 ± 0.19
10	propionic	-6.47	-5.31 ± 0.19	-5.19 ± 0.17
11	propane-2-methoxy-2-methyl	-0.79	-0.44 ± 0.21	-0.43 ± 0.20
12	propionitrile	-3.85	-3.39 ± 0.17	-3.25 ± 0.15
13	trimethylamine	-3.42	-2.35 ± 0.17	-1.67 ± 0.18
	average unsigned error (AUE)		1.08	1.17
	R^2		0.96	0.95
	slope		0.96	0.97
	intercept		0.89	0.96

^a The 5- λ schedule corresponds to the default coupling scheme. All the energies are reported in kcal/mol.

chemical structures for all molecules within each of the groups are available from the Supporting Information (Figure S2).

Subset of Molecules for Solvent Model and Charge Assignment Comparison. A subset of 13 molecules was initially investigated to study effects of the solvent model and the charge assignment method. This subset was chosen by applying hierarchical clustering to the Tanimoto similarity matrix⁵⁴ derived from linear 2D molecular fingerprints, as implemented in Canvas.²⁶ From the initial 239 compounds in Table 2, one compound (the closest member to the cluster centroid) from each of 13 clusters was chosen (Table 3). Three different solvent models were compared here—SPC,⁵⁵ TIP3P,⁵⁶ and TIP4P.⁵⁶ The SPC and TIP3P are commonly

used three-site water models that differ in potential terms and geometry. TIP4P is a commonly used 4-site water model that places negative charge on a dummy atom near the oxygen along the bisector of the H—O—H angle.

Results and Discussions

Solvent Models. The absolute solvation free energies using the SPC, TIP3P, and TIP4P water models for the 13 molecule subset (see Methods Section) are shown in Table 3. For completeness, the absolute solvation free energies were also calculated for a set of five molecules that represents neutral amino acid side chain analogues Glu, Tyr, Asp, His, and Phe (Table 3). The statistical uncertainty of the computed

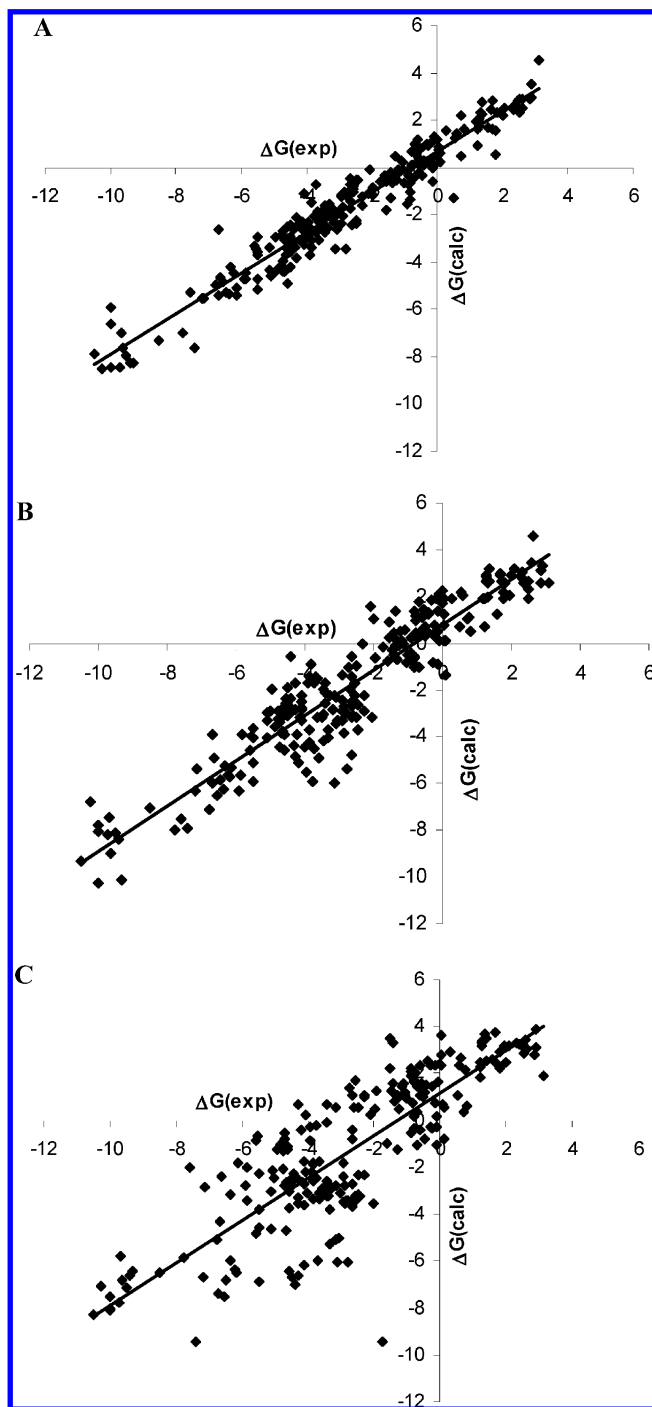


Figure 2. Plot of predicted versus experimental solvation free energy (in kcal/mol) using different force fields. (A) OPLS_2005, (B) AM1-BCC charges with GAFF vdW and bonded parameters (AM1-BCC/GAFF), and (C) CHelpG charges with CHARMM-MSI vdW and bonded parameters (CHelpG/CHARMM-MSI).

free energy is estimated using the subsampling bootstrap method as described in the Theory Section. OPLS_2005 parameters and charges were used for all molecules. The calculations on this subset of molecules were performed in order to find a good solvent model for further analysis on the full data set and were not intended as a complete study.

The correlation coefficient (R^2) between the experimental and the predicted solvation free energies using SPC, TIP3P, and TIP4P water models is 0.96, 0.96, and 0.92, respectively,

Table 5. Absolute Solvation Free Energies using a Modified λ Coupling Parameter for vdW^a

entry ID	title	exp	λ_{vdW}^9	$\Lambda_{\text{vdW}}^{13}$
1	anthracene	-4.23	-3.06 ± 0.23	-2.87 ± 0.25
2	biphenyl	-2.64	-1.40 ± 0.24	-1.52 ± 0.25
3	nitrobenzene	-4.12	-2.61 ± 0.19	-2.30 ± 0.16

^a The 9- λ schedule corresponds to the default coupling scheme. All the energies are reported in kcal/mol.

for the small molecules reported in Table 3. In general, the solvent models perform comparably across this subset of molecules, and the same compounds present a challenge for all of the water models. These results suggest that there is not an extreme sensitivity to the choice of water model, at least for the current subset, representing small molecules. For amino acid side chain analogues (Table 3), the R^2 between the experimental and the predicted solvation free energy using SPC, TIP3P, and TIP4P water models is 0.95, 0.91, and 0.96, respectively. For the amino acid analogues, the TIP4P solvent model shows the lowest average unsigned error (AUE). This is in accordance with the previously published work where it has been reported that the hydration free energies of various small molecules in explicit solvent could be water-model dependent.¹⁵ However, we chose to use the SPC model for the remaining calculations in this work because it has the lowest AUE, the best R^2 , a good slope, and the smallest maximum error for the 13 small molecule subset and has similarly good results for the amino acid side chain analogues. Furthermore, simulations run faster with a three-point water model, like SPC, as compared to a four-point model, like TIP4P.

Effect of Additional λ Windows. The alchemical transformations presented in this work use a 5- λ schedule with linear scaling ($\lambda_{\text{coul}}^5 = 0.0, 0.25, 0.5, 0.75$, and 1) for the electrostatic component of the solvation free energy. To our knowledge, there has been no direct study reported in the literature to optimize the electrostatic λ schedule. Work by Deng and Roux⁵² uses an 11- λ schedule ($\lambda_{\text{coul}}^{11} = 0.0, 0.1, 0.2, 0.3, 0.4, 0.5, 0.6, 0.7, 0.8, 0.9$, and 1) to linearly scale the electrostatics, whereas Mobley et al¹⁵ uses a 5- λ schedule. A reduced number of λ windows is desirable to speed the calculations but has the potential to produce inaccurate results.

The results for the 13-compound subset using the 5- and 11- λ schedules are shown in Table 4. The solvation free energies are equivalent within the errors of the computation, suggesting that the reduced λ_{coul}^5 schedule is sufficient for the calculation of absolute solvation free energies of typical small organic molecules. The correlation with experiment (R^2) is 0.95 and 0.96 for λ_{coul}^5 and $\lambda_{\text{coul}}^{11}$ schedules, respectively (Table 4).

In the current alchemical transformation protocol, the vdW component of the solvation free energy is staged using a 9- λ coupling parameters ($\lambda_{\text{vdW}}^9 = 0.0, 0.1069742, 0.1745536, 0.2252634, 0.2816288, 0.366175, 0.5014272, 0.7099106$, and 1.0). As a test, we added four additional λ windows near $\lambda = 0.0$, since this is believed to be the most critical part of the λ schedule due to the effective appearance of new excluded volume regions. The resulting 13- λ schedule had

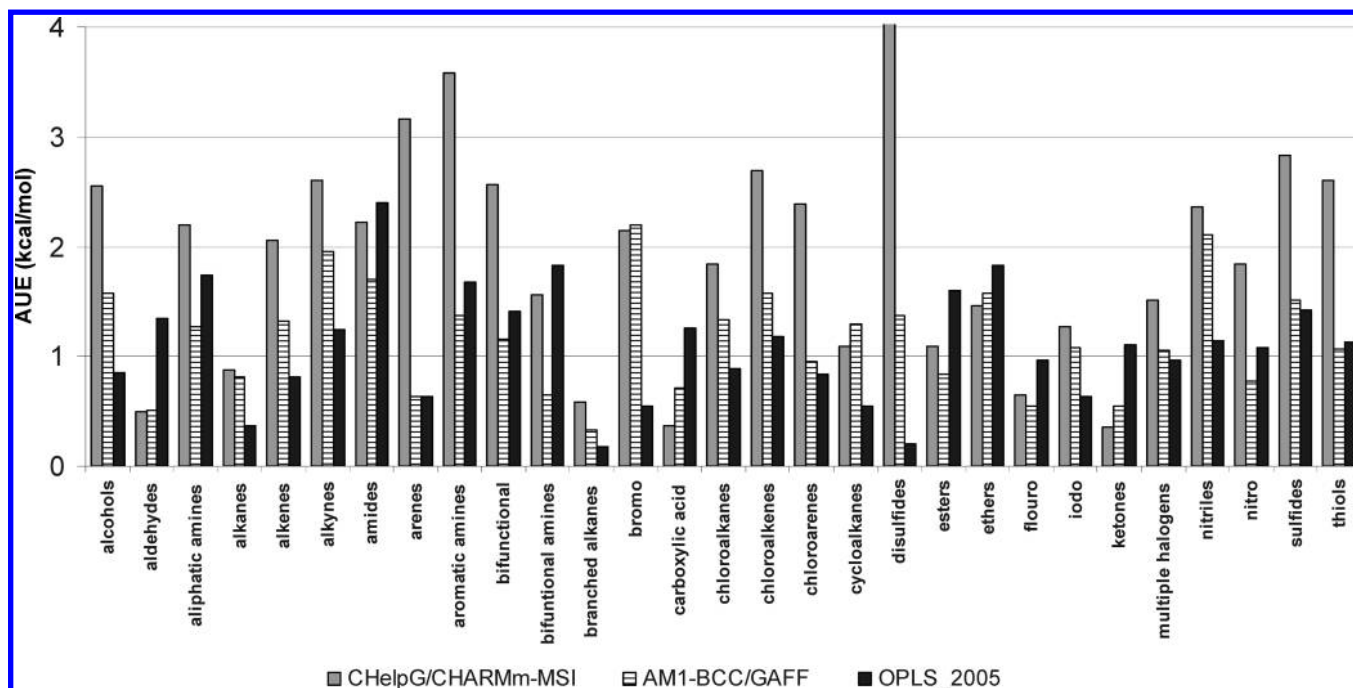


Figure 3. Comparison of the average unsigned error (AUE) for different classes of compounds using OPLS_2005, AM1-BCC/GAFF, and CHelpG/CHARMM-MSI.

λ values of $\lambda_{\text{vdw}}^{13} = 0.0, 0.01, 0.02, 0.05, 0.07, 0.1069742, 0.1745536, 0.2252634, 0.2816288, 0.366175, 0.5014272, 0.7099106$, and 1.0 . We ran the new λ schedule on three of the bulkier molecules in order to stress the difference in the vdW treatment, which should be more significant with larger molecules. As seen in Table 5, the results from the default (λ_{vdw}^9) and modified ($\lambda_{\text{vdw}}^{11}$) λ schedules are essential equivalent within the statistical error range.

Comparison of the Force Fields. Two different charge models were used for calculating the absolute solvation free energies on the 13 compound subset—default OPLS_2005 charges with the OPLS_2005 force field (OPLS_2005/OPLS_2005) and AM1-BCC charges with the OPLS_2005 force field (AM1-BCC/OPLS_2005). The OPLS_2005 charges were assigned using the default Schrödinger atom-typing infrastructure.²⁶ The AM1-BCC charges were taken from

Shivakumar et al.¹⁸ AM1-BCC was chosen for comparison because it outperformed the other charge models discussed in the work by Shivakumar et al. Finally, the best combined charge assignment method and force field from Shivakumar et al. (AM1-BCC/GAFF) was also added to the comparison. The results are shown in Table 6. The OPLS_2005/OPLS_2005 combination performs better than either AM1-BCC/GAFF or AM1-BCC/OPLS_2005, although the latter is very close. The correlation coefficient R^2 is 0.96 for OPLS_2005/OPLS_2005, whereas it is 0.95 for AM1-BCC/OPLS_2005 and 0.87 for AM1-BCC/GAFF. However, the AM1-BCC/OPLS_2005 has the lowest AUE and best slope among the three. This shows that the AM1-BCC charge model, which has been often used in conjunction with GAFF, also performs equally well with the OPLS_2005 force field. The major outlier in AM1-BCC/OPLS_2005 and AM1-BCC/

Table 6. Comparison of the Force Fields and Charge Assignment Methods (OPLS_2005/OPLS_2005, AM1-BCC/OPLS_2005, and AM1-BCC/GAFF)^a

entry ID	title	exp	OPLS_2005/OPLS_2005	AM1-BCC/OPLS_2005	AM1-BCC/GAFF ^b
1	1,3-dioxolane	−4.10	−2.50 ± 0.21	−3.98 ± 0.18	−2.81
2	4-methyl-1H-imidazole	−10.25	−8.50 ± 0.21	−8.37 ± 0.20	−6.80
3	biphenyl	−2.64	−1.40 ± 0.24	−2.63 ± 0.21	−2.68
4	butanal	−3.18	−1.80 ± 0.18	−3.51 ± 0.18	−2.85
5	cyclopropane	0.75	2.18 ± 0.17	2.20 ± 0.11	1.10
6	dimethyldisulfide	−1.54	−1.28 ± 0.18	−0.58 ± 0.24	0.23
7	morpholine	−7.17	−5.54 ± 0.25	−5.47 ± 0.17	−6.34
8	nitrobenzene	−4.12	−2.61 ± 0.19	−4.37 ± 0.17	−3.18
9	piperazine	−7.40	−7.63 ± 0.21	−7.17 ± 0.20	−7.94
10	propionic	−6.47	−5.31 ± 0.19	−6.96 ± 0.19	−5.84
11	propane,2-methoxy-2-methyl	−0.79	−0.44 ± 0.21	−0.98 ± 0.25	−0.11
12	propionitrile	−3.85	−3.39 ± 0.17	−0.91 ± 0.18	−1.43
13	trimethylamine	−3.42	−2.35 ± 0.17	−2.25 ± 0.17	−1.71
	average unsigned error (AUE)		1.08	0.90	1.15
	R^2		0.96	0.94	0.87
	slope		0.96	0.95	0.89
	intercept		0.89	0.49	0.60

^a The SPC water model was used for all simulations. Energies are reported in kcal/mol. ^b Obtained from Shivakumar et al.¹⁸

Molecule name	Experimental Solvation Free Energies	OPLS 2005 Charges and Solvation Free Energies	CM1A-BCC/OPLS_2005 Charges and Solvation Free Energie
N,N- dimethylacetamide	-8.50 kcal/mol		
		-6.16 ± 0.19 kcal/mol	-7.31 ± 0.21 kcal/mol
methoxybenzene	-3.73 kcal/mol		
		-0.72 ± 0.22 kcal/mol	-3.86 ± 0.16 kcal/mol
N,N- diethylethanamine	-4.07 kcal/mol		
		-1.07 ± 0.19 kcal/mol	-4.42 ± 0.22 kcal/mol
acetaldehyde	-3.5 kcal/mol		
		-2.10 ± 0.17 kcal/mol	-3.55 ± 0.12 kcal/mol

Figure 4. Partial atomic charges and solvation free energies in kcal/mol for a selection of polar compounds (amide, ether, amine, and aldehyde) using OPLS_2005 and CM1A-BCC/OPLS_2005.

GAFF is propionitrile, which performs much better using OPLS_2005/OPLS_2005. This suggests further improvement in the AM1-BCC charges for nitrile functional groups. A similar observation was also made in the published work of Shivakumar et al.

Absolute Solvation Free Energies of the Full Test Set

Finally, we calculate the absolute solvation free energy for the entire set of 239 molecules using the SPC water model and the OPLS_2005 force field. The AUE for OPLS_2005 is 1.10, which is consistent with the results from the 13-compound diverse subset shown in Table 6. The AUE as reported by Shivakumar et al. was 1.17 for AM1-BCC/GAFF

and 1.88 for CHelpG/CHARMm-MSI. Figure 2A shows the correlation between the predicted and experimental absolute solvation free energies, with a coefficient (R^2) of 0.94, a slope of 0.86, and an intercept of 0.68 kcal/mol. The correlation is significantly better than that for AM1-BCC/GAFF (Figure 2B) or CHelpG/CHARMm-MSI (Figure 2C) on the same set of molecules. The R^2 , slope, and intercept for AM1-BCC/GAFF were 0.87, 0.97, and 0.78 and for CHelpG/CHARMm-MSI were 0.72, 0.91, and 1.19, respectively.

To further compare the performance of different charge models and force fields, the compounds were analyzed based on the chemical functional group classes shown in Table 2. The AUE in the absolute solvation free energy for each class is shown in Figure 3. The OPLS_2005 force field produces

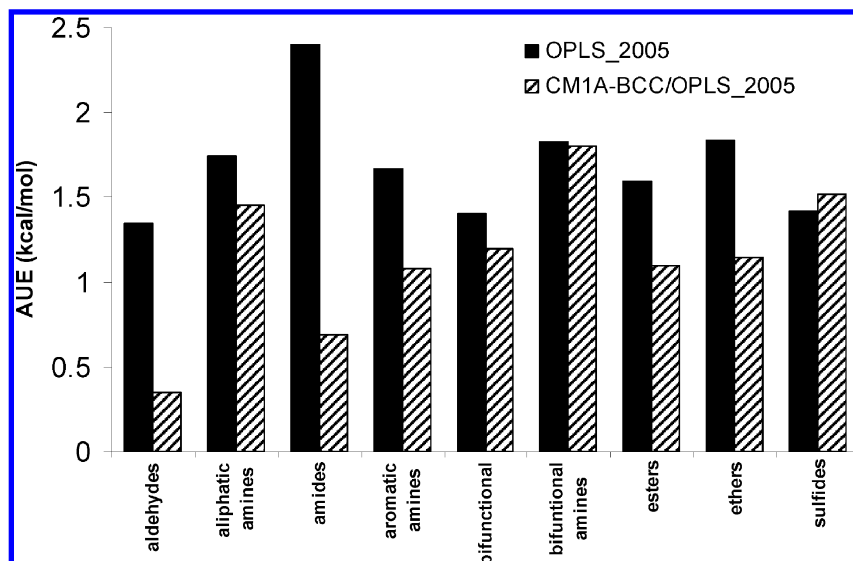


Figure 5. AUE using the OPLS_2005 and CM1A-BCC/OPLS_2005 force fields for the functional group classes that perform poorly with the OPLS_2005 force field.

the lowest AUE for a number of important functional groups, such as alcohols, alkanes, alkenes, cycloalkanes, and disulfides. Both OPLS_2005 and AM1-BCC/GAFF perform similarly for other hydrocarbon groups (branched alkanes, alkynes, and cycloalkanes), polar groups (aldehydes, ketones, carboxylic acids, esters, ethers, aliphatic amines, nitro, and sulfides), and the majority of the halogenated molecules. The worst performing classes of compounds with OPLS_2005 contain polar functional groups, such as amides, amines, esters, and ethers. CHelpG/CHARMM-MSI did not perform well on many systems, with 14 classes having an AUE of greater than 2.0 kcal/mol and 3 classes (arenes, amines, and disulfides) having an AUE greater than 3.0 kcal/mol.

OPLS_2005 with CM1A-BCC Charges. Overall, the absolute solvation free energies obtained using the OPLS_2005 force field show the highest correlation with the experimental solvation free energies compared to other two force fields mentioned in this study. However, there are classes of compounds with large errors that need improvement even with OPLS_2005. For example, the nitrogen-containing polar functional groups, such as amines and amides, did not perform well with OPLS_2005. Polar functional groups like these have previously posed challenges in predicting solvation free energies with fixed charge force fields.⁵⁷ Interestingly, these functional groups performed better using the semiempirical AM1-BCC charges in the work by Shivakumar et al.,¹⁸ suggesting that an improved charge assignment model could lead to better OPLS_2005 predictions.

We examined the most challenging compound classes using the CM1A-BCC charge assignment method with the OPLS_2005 force field. The partial atomic charges for a subset of molecules from OPLS_2005 and CM1A-BCC are shown in Figure 4 to illustrate the subtle differences in atomic charges and how they impact the solvation free energies. For example, the experimental solvation free energy for *N,N*-dimethylacetamide is -8.5 kcal/mol. Using the default charges from the OPLS_2005 force field, the predicted absolute solvation free energy is -6.16 ± 0.19 kcal/mol, whereas using CM1A-BCC charges, we see an improvement

in the predicted absolute solvation free energy to -7.31 ± 0.21 kcal/mol that results from a series of small charge differences spread across the molecule. The absolute solvation free energies using OPLS_2005 are systematically less negative than the experimental values for these polar molecules, whereas the CM1A-BCC charges result in a more favorable predicted solvation free energy. Significant improvements are also observed with other functional classes, such as ethers, amines, and aldehydes. A representative molecule from each of these classes is shown in Figure 4. The Figure 5 shows the AUE in the solvation free energy using CM1A-BCC charges for the compound classes that perform poorly with the default OPLS_2005 force field charge assignment. The results for CM1A-BCC charges are better in all cases, except sulfides where they are marginally worse. There are significant improvements for aldehydes, amides, aromatic amines, esters, and ethers functional groups.

Conclusions

In this study we computed the absolute solvation free energies for a diverse set of 239 neutral molecules using molecular dynamics/free energy perturbation (MD/FEP) with explicit solvent and compared the results with experimental data. The OPLS_2005 all-atom force field performed well compared with two other commonly used small molecule force fields (AM1-BCC/GAFF and CHelpG/CHARMM-MSI) that have been previously reported¹⁸ for the same set of small molecules. While there was good correlation with experimental values and a low average unsigned error across the entire set with the OPLS_2005 force field, there were important classes of polar compounds that performed sub-optimally. It was found that for most polar classes of compounds the results improved when the newly developed CM1A-BCC charge assignment methodology was used in conjunction with the rest of the OPLS_2005 force field parameters. Further work is needed to explore the effects across all classes of compounds, including nonpolar functional groups. While the CM1A-BCC charges described in

this work performed well when combined with the other OPLS_2005 force field parameters, a self-consistent force field will likely perform better. We are in the process of completing the development of the next generation OPLS-AA force field, which uses the CM1A-BCC charge assignment method described in this work and also greatly expands on the parameter space coverage of small molecules compared to the OPLS_2005 force field. Validation of the complete force field for solvation free energy calculations will be reported in a future work.

The accurate characterization of solvation effects is critical in the thermodynamic process of protein–ligand binding. The prediction of solvation free energies provides a surrogate for the biologically relevant process of transferring a small molecule from solution (high-dielectric environment) to the binding site of a protein (low-dielectric region) and, therefore, is an important step toward predicting accurate binding free energies. Further work on improving force field accuracy and enhanced sampling simulation methods could help to bring the accuracy level of binding free energy predictions to the point where they can provide substantial value in the drug discovery arena.

Acknowledgment. The authors thank Drs. Huafeng Xu, Byungchan Kim, Teng Lin, and David Rinaldo for helpful discussions and suggestions and Drs. Ramy Farid and Ken Dyall for providing critical comments on the manuscript. Also, the authors thank Profs. Benoit Roux and Bill Jorgensen for helpful discussions concerning the FEP methodology.

Supporting Information Available: Variation in RMSE as a function of simulation time (Figure S1) and the 2D chemical structures for all molecules used in this study along with their experimental and calculated solvation free energies (Figure S2) is available. The coordinates of the individual molecules can be requested from the authors or downloaded from <http://www.schrodinger.com>. This material is available free of charge via the Internet at <http://pubs.acs.org>.

References

- Jorgensen, W. L. *Science* **2004**, *303*, 1813–1818.
- Karplus, M. *Acc. Chem. Res.* **2002**, *35*, 321–323.
- Shoichet, B. K.; Leach, A. R.; Kuntz, I. D. *Proteins: Struct., Funct., Genet.* **1999**, *34*, 4–16.
- Eisenberg, D.; McLachlan, A. D. *Nature* **1986**, *319*, 199–203.
- Kirkwood, J. G. *J. Chem. Phys.* **1935**, 300–313.
- Zwanzig, R. W. *J. Chem. Phys.* **1954**, *22*, 1420–1426.
- Still, W. C.; Tempczyk, A.; Hawley, R. C.; Hendrickson, T. *J. Am. Chem. Soc.* **1990**, *112*, 6127–6129.
- Cramer, C. J.; Truhlar, D. G. *Chem. Rev.* **1999**, *99*, 2161–2200.
- Sharp, K. A.; Honig, B. *Annu. Rev. Biophys. Biophys. Chem.* **1990**, *19*, 301–332.
- Nina, M.; Beglov, D.; Roux, B. *J. Phys. Chem. B* **1997**, *101*, 5239–5248.
- Roux, B.; Simonson, T. *Biophys. Chem.* **1999**, *78*, 1–20.
- Kollman, P. *Chem. Rev.* **1993**, *93*, 2395–2417.
- Jorgensen, W. L. *Acc. Chem. Res.* **1989**, *22*, 184–189.
- Jorgensen, W. L.; Ravimohan, C. *J. Chem. Phys.* **1985**, *83*, 3050–3054.
- Mobley, D. L.; Dumont, E.; Chodera, J. D.; Dill, K. A. *J. Phys. Chem. B* **2007**, *111*, 2242–2254.
- Mobley, D. L.; Dill, K. A.; Chodera, J. D. *J. Phys. Chem. B* **2008**, *112*, 938–946.
- Nicholls, A.; Mobley, D. L.; Guthrie, J. P.; Chodera, J. D.; Bayly, C. I.; Cooper, M. D.; Pande, V. S. *J. Med. Chem.* **2008**, *51*, 769–779.
- Shivakumar, D.; Deng, Y.; Roux, B. *J. Chem. Theory Comput.* **2009**, *5*, 919–930.
- Van Der Spoel, D.; Lindahl, E.; Hess, B.; Groenhof, G.; Mark, A. E.; Berendsen, H. J. C. *J. Comput. Chem.* **2005**, *26*, 1701–1718.
- Wang, J.; Wolf, R. M.; Caldwell, J. W.; Kollman, P. A.; Case, D. A. *J. Comput. Chem.* **2004**, *25*, 1157–1174.
- Momany, F. A.; Rone, R. *J. Comput. Chem.* **1992**, *13*, 888–900.
- Jakalian, A.; Bush, B. L.; Jack, D. B.; Bayly, C. I. *J. Comput. Chem.* **2000**, *21*, 132–146.
- Breneman, C. M.; Wiberg, K. B. *J. Comput. Chem.* **1990**, *11*, 361–373.
- Bayly, C. I.; Cieplak, P.; Cornell, W. D.; Kollman, P. A. *J. Phys. Chem.* **1993**, *40*, 10269–10280.
- Storer, J. W.; Giesen, D. J.; Cramer, C. J.; Truhlar, D. G. *J. Comput.-Aided Mol. Des.* **1995**, *9*, 87–110.
- Maestro, version 8.5; Schrodinger, Inc.: New York, NY, 2008.
- Desmond Molecular Dynamics System; D. E. Shaw Research: New York, NY, 2008.
- Bowers, K. J.; Chow, E.; Xu, H.; Dror, R. O.; Eastwood, M. P.; Gregerson, B. A.; Klepeis, J. L.; Kolossvary, I.; Moraes, M. A.; Sacerdoti, F. D.; Salmon, J. K.; Shan, Y.; Shaw, D. E. *Scalable Algorithms for Molecular Dynamics Simulations on Commodity Clusters*; Proceedings of the ACM/IEEE Conference on Supercomputing (SC06) Tampa, FL 2006.
- Shaw, D. E. *J. Comput. Chem.* **2005**, *26*, 1318–1328.
- Bowers, K. J.; Dror, R. O.; Shaw, D. E. *J. Chem. Phys.* **2006**, *124*, 184109–184111.
- Lippert, R. A.; Bowers, K. J.; Dror, R. O.; Eastwood, M. P.; Gregersen, B. A.; Klepeis, J. L.; Kolossvary, I.; Shaw, D. E. *J. Chem. Phys.* **2007**, *126*, 046101–046102.
- Essmann, U.; Perera, L.; Berkowitz, M.; Darden, T.; Lee, H.; Pedersen, L. *J. Chem. Phys.* **1995**, *103*, 8577–8593.
- Beutler, T. C.; Mark, A. E.; Schaik, R. C.; Gerber, P. R.; van Gunsteren, W. F. *Chem. Phys. Lett.* **1994**, *222*, 529–643.
- Lague, P.; Pastor, R. W.; Brooks, B. R. *J. Phys. Chem. B* **2003**, *108*, 363–368.
- Bennett, C. H. *J. Comput. Phys.* **1976**, *22*, 245–268.
- Chernick, M. R. *Bootstrap Methods: A Guide for Practitioners and Researchers*, 2nd ed.; Wiley: Hoboken, NJ, 2007.
- Banks, J. L.; Beard, H. S.; Cao, Y.; Cho, A. E.; Damm, W.; Farid, R.; Felts, A. K.; Halgren, T. A.; Mainz, D. T.; Maple, J. R.; Murphy, R.; Philipp, D. M.; Repasky, M. P.; Zhang, L. Y.; Berne, B. J.; Friesner, R. A.; Gallicchio, E.; Levy, R. M. *J. Comput. Chem.* **2005**, *26*, 1752–1780.

- (38) Jacobson, M. P.; Kaminski, G. A.; Rapp, C. A.; Friesner, R. A. *J. Phys. Chem. B* **2002**, *106*, 11673–11680.
- (39) Jensen, K. P.; Jorgensen, W. L. *J. Chem. Theory Comput.* **2006**, *2*, 1499–1509.
- (40) Kaminski, G.; Friesner, R. A.; Tirado-Rives, J.; Jorgensen, W. L. *J. Phys. Chem. B* **2001**, *105*, 6474–6487.
- (41) Jorgensen, W. L.; Maxwell, D. S.; Tirado-Rives, J. *J. Am. Chem. Soc.* **1996**, *118*, 11225–11236.
- (42) Damm, W.; Frontera, A.; Tirado-Rives, J.; Jorgensen, W. L. *J. Comput. Chem.* **1997**, *18*, 1955–1970.
- (43) Jorgensen, W. L.; McDonald, N. A. *J. Phys. Chem. B* **1998**, *102*, 8049–8059.
- (44) Rizzo, R. C.; Jorgensen, W. L. *J. Am. Chem. Soc.* **1999**, *121*, 4827–4836.
- (45) Price, M. L. P.; Ostrovsky, D.; Jorgensen, W. L. *J. Comput. Chem.* **2001**, *22*, 1340–1352.
- (46) Jakalian, A.; Jack, D. B.; Bayly, C. I. *J. Comput. Chem.* **2002**, *23*, 1623–1641.
- (47) Chambers, C. C.; Hawkins, G. D.; Cramer, C. J.; Truhlar, D. G. *J. Phys. Chem.* **1996**, *100*, 16385–16398.
- (48) Udier-Blagovic, M.; De Tirado, P. M.; Pearlman, S. A.; Jorgensen, W. L. *J. Comput. Chem.* **2004**, *25*, 1322–1332.
- (49) Schlick, T. *Molecular modeling and simulation: an interdisciplinary guide*; Springer: New York, NY, 2002.
- (50) Martyna, G. J.; Klein, M. L.; Tuckerman, M. J. *J. Chem. Phys.* **1992**, *97*, 2635–2643.
- (51) Martyna, G. J.; Tobias, D. J.; Klein, M. L. *J. Chem. Phys.* **1994**, *101*, 4177–4189.
- (52) Deng, Y.; Roux, B. *J. Phys. Chem. B* **2004**, *108*, 16567–16576.
- (53) Maple, J. R.; Cao, Y.; Damm, W.; Halgren, T. A.; Kaminski, G. A.; Zhang, L. Y.; Friesner, R. A. *J. Chem. Theory Comput.* **2005**, *1*, 694–715.
- (54) Tanimoto, T. T. *IBM Internal Report*; IBM: Armonk, NY 1957.
- (55) Berendsen, H. J. C.; Grigera, J. R.; Straatsma, T. P. *J. Phys. Chem.* **1987**, 6269–6271.
- (56) Jorgensen, W. L.; Chandrasekhar, J.; Madura, J. D.; Impey, R. W.; Klein, M. L. *J. Chem. Phys.* **1983**, *79*, 926–935.
- (57) Morgantini, P.-Y.; Kollman, P. A. *J. Am. Chem. Soc.* **2002**, *117*, 6057–6063.

CT900587B